Chapter 1

Introduction

This thesis addresses the problem of building an anisotropic velocity model using Full Waveform Inversion (FWI). In exploration geophysics, velocity is crucial in many stages of a processing workflow, especially in creating an accurate image of the subsurface. A good velocity model helps correctly position the geological interfaces and focus the reflections. Among a number of velocity model building techniques, FWI is a powerful method that can theoretically recover all wavelength components of the velocity by directly matching the simulated seismic data and the observed data (Tarantola, 1984; Pratt, 1999; Virieux and Operto, 2009). Developments in seismic acquisition led to the recording of three dimensional wide azimuth and long offset data. When multiple azimuths and offsets are inverted together, directional velocity variation, aka. anisotropy, needs to be accounted for. Studies have shown that FWI gives better results with anisotropy (Barnes et al., 2008; Lee et al., 2010; Prieux et al., 2011). Isotropic FWI on data that exhibit anisotropy can result in incorrect velocity models, and therefore misposition reflectors and create incoherent images.

The simplest type of anisotropy is vertical transverse isotropy (VTI), which is commonly found in areas of horizontally deposited layers. Even though, the thickness of individual, possibly isotropic, layers is smaller than the dominant seismic wavelength,

the effective medium is anisotropic due to the discrepancy between vertical and horizontal velocities (Backus, 1962). There is a symmetry axis that is perpendicular to the bedding. Seismic velocity depends on the angle between propagation direction and this symmetry axis (Figure 1.1). Waves that travel along the bedding planes share the same velocity while those that propagate along the symmetry axis are slower. To describe a VTI medium requires *five* elastic coefficients (besides density). Under the pseudo-acoustic assumption, the number of independent parameters reduces to *three*. This is also the assumption I make in this thesis.

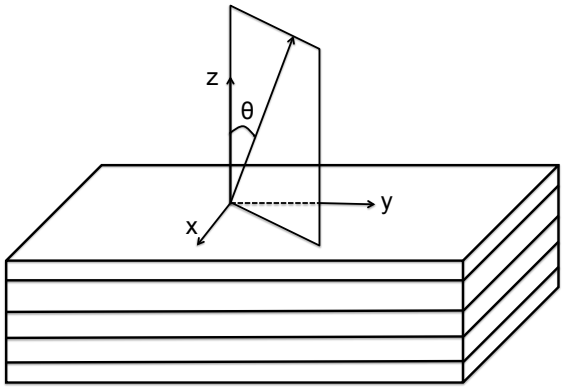

Figure 1.1: Schematic illustration of a VTI medium.

FWI is a nonlinear and under-determined inverse problem. Incorporating anisotropy introduces additional parameters (the anisotropic parameters) and makes the problem even more difficult. Firstly, these anisotropic parameters are less sensitive to surface seismic data than velocity. This implies that the anisotropic FWI problem is more ill-conditioned than the isotropic problem. Secondly, there are trade-offs between velocity and anisotropic parameters, meaning that there are multiple subsurface models that could fit the data equally well. This thesis presents a method to reduce the nonuniqueness and uncertainty in anisotropic FWI by constraining the inversion with information derived from pore pressure and rock physics principles.

A NONUNIQUE PROBLEM

I here illustrate the nonuniqueness in anisotropic velocity model building with a simple NMO exercise (more examples are presented in Chapter 3). Two parameters that control the moveout in a layered VTI medium are NMO velocity v_n and η (Alkhalifah and Tsvankin, 1995), which are related to vertical velocity v_z and the two Thomsen parameters ϵ and δ (Thomsen, 1986) by

$$v_n = v_z\sqrt{1+2\delta}, \tag{1.1a}$$

$$\eta = \frac{\epsilon-\delta}{1+2\delta}. \tag{1.1b}$$

The NMO equation is

$$t^2 = t_0^2 + \frac{x^2}{(v_n^{RMS})^2} - \frac{2\eta^{RMS}x^4}{(v_n^{RMS})^2\left[t_0^2(v_n^{RMS})^2 + (1+2\eta^{RMS})x^2\right]}, \tag{1.2}$$

in which the RMS v_n and η can be computed using Dix equations

$$(v_n^{RMS})^2 = \frac{1}{t_0}\sum_i (v_n^{(i)})^2 t_0^{(i)}, \tag{1.3a}$$

$$(v_n^{RMS})^4(1+8\eta^{RMS}) = \frac{1}{t_0}\sum_i (v_n^{(i)})^4(1+8\eta^{(i)})t_0^{(i)}, \tag{1.3b}$$

$$t_0 = \sum_i t_0^{(i)}, \tag{1.3c}$$

with $v_n^{(i)}$, $\eta^{(i)}$, and $t_0^{(i)}$ being the interval NMO velocity, η, and zero-offset two-way travel time (Tsvankin, 2012). In the NMO equation (Equation 1.2), η only appears in the fourth order term (x^4), meaning that small offset moveout is mainly controlled by NMO velocity while long offset moveout is controlled by both NMO velocity and η.

Figure 1.2(a) shows a three layer velocity model denoted with interval and RMS values of velocity and anisotropic parameters. One seismic source and a receiver array are placed on the surface. The synthetic recorded data are shown in Figure 1.2(b).

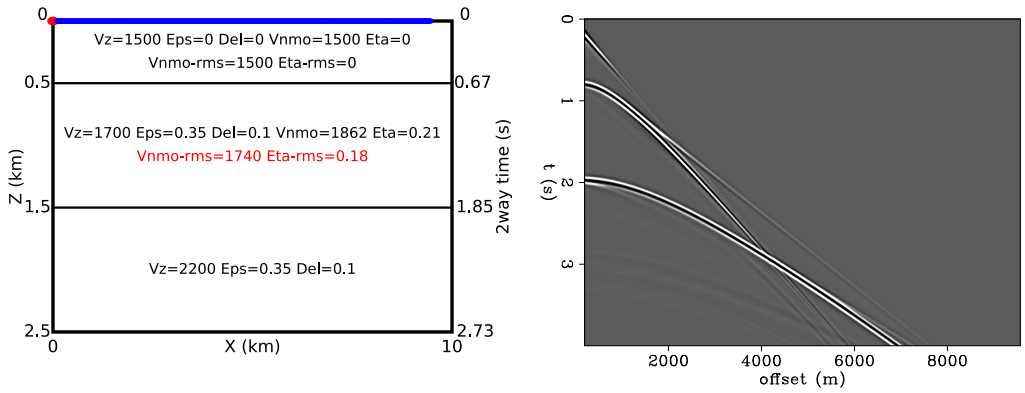

(a) (b)

Figure 1.2: (a) A three layer velocity model denoted with interval and RMS values, a source (red dot), a receiver array (in blue). (b) Synthesized recorded data.

The focus is on the reflection at the bottom of the second layer, whose RMS values are $v_n^{RMS} = 1740$ m/s and $\eta^{RMS} = 0.18$, that arrives at around 2 seconds at the nearest offset. Figure 1.3(a) shows the data corrected with the wrong NMO velocity and true η. As a result of having the wrong NMO velocity, the reflection event is not flattened at any offset, even with the correct η. Figure 1.3(b) shows the result with correct NMO velocity and wrong η. Having the correct velocity flattens the reflection at near offset (upto 2 km). These observations are consistent with what described above by the NMO equation (Equation 1.2). Figure 1.4(a) shows the NMO'ed data with both correct velocity and η while 1.4(b) is the result for incorrect parameters. In these figures, the flatness of the reflection event is approximately the same. The semblance panel (Figure 1.5) demonstrates the problem more clearly: high stacking energy can be achieved with either large NMO velocity and small η or small NMO velocity and large η. This illustrates the nonuniqueness in anisotropic velocity model building. Similar illustrations are also shown in Plessix and Cao (2011) for FWI and in Li et al. (2016a) for Wave Equation Migration Velocity Analysis (WEMVA).

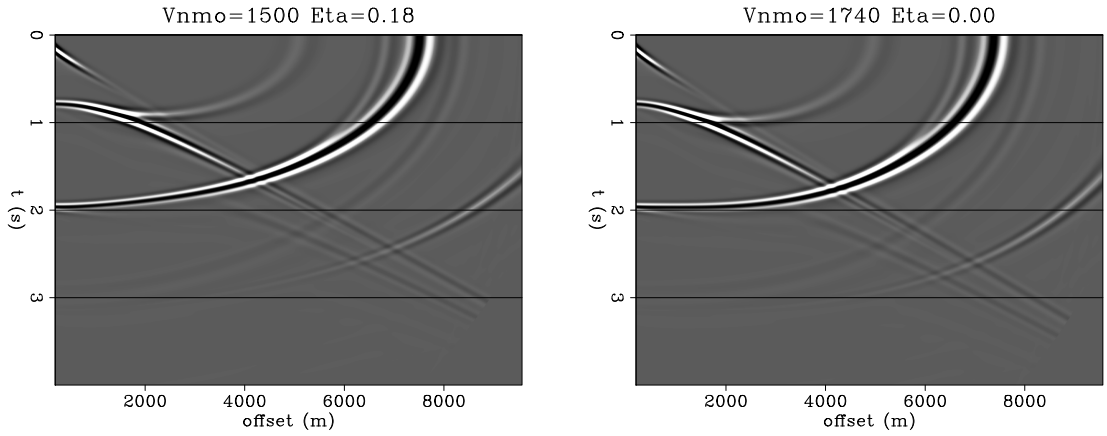

(a) (b)

Figure 1.3: Anisotropic NMO with: (a) correct RMS v_n and wrong η and (b) wrong RMS v_n and correct η.

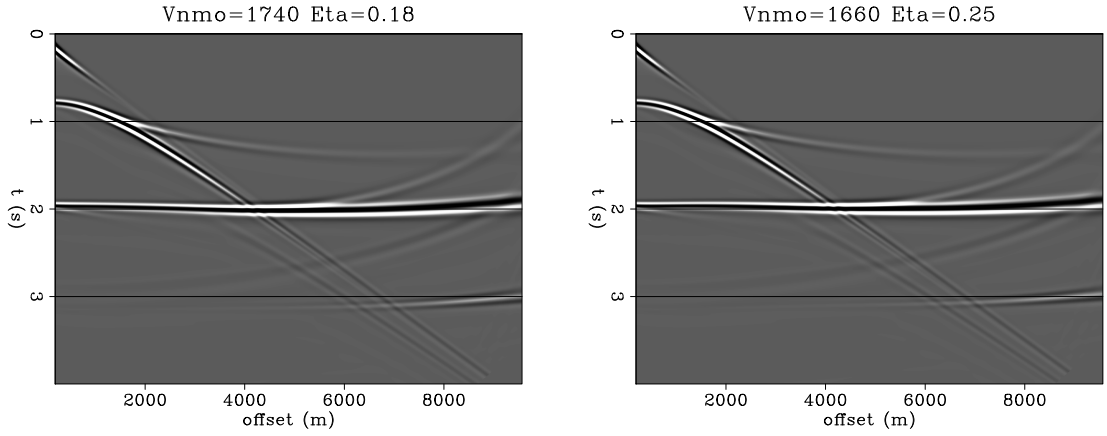

(a) (b)

Figure 1.4: Anisotropic NMO with: (a) correct RMS v_n and correct η and (b) wrong RMS v_n and wrong η.

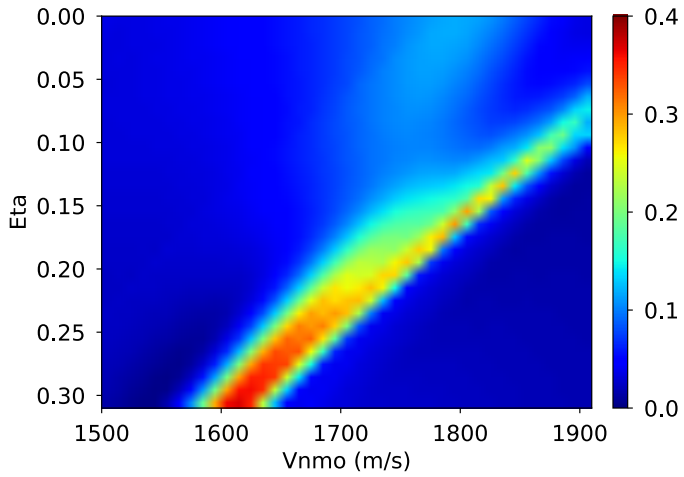

Figure 1.5: Semblance computed from NMO analysis of both v_n and η on the reflection event at 2 second shown in Figure 1.2(b).

OVERVIEW OF THESIS

The thesis is organized as followed:

Theory and formulation

Chapter 2 presents the VTI pseudo-acoustic anisotropic wave equations that are used to model seismic data, defines an FWI objective function, applies adjoint state methods to derive the gradients and Hessian matrix, and analyzes the stability of the equations. I show that anisotropic FWI is most conveniently and compactly represented in terms of stiffness coefficients from which any other parameterizations can be derived using chain rules. The correct adjoint system of the pseudo-acoustic anisotropic wave equations is unstable and this chapter presents a possible solution to this problem. Surprisingly, synthetic tests demonstrate that a more cost-effective solution is to simply use the time-reversed forward equations, which is shown not to negatively affect the convergence of FWI.

Sensitivity and parameterization

Chapter 3 is a study on sensitivity and parameterization of anisotropic FWI. From a number of synthetic experiments, I observe that using one velocity and two anisotropic parameters results in the best recovered models and final migrated images. When a combination of this type is used, velocity is the most sensitive parameter and therefore is the most updated. Updates in the other two anisotropic parameters are much less significant and heavily suffer from velocity crosstalk. Experiments with Newton's methods seems to suggest that both the full Hessian and the Gauss-Newton Hessian matrices fail to resolve the crosstalk between velocity and anisotropic parameters. Despite being less reliably recovered, including anisotropy in FWI leads to better final velocity models.

Rock physics guided velocity model building

Chapter 4 describes a rock physics workflow that can be used to build a velocity model in a VTI medium. This workflow combines well logs, drilling data, basin history, shale diagenesis, and rock physics principles to model the relationship between velocity and pore pressure. The inspiration comes from the fact that in a shale-rich environment like the Gulf of Mexico, in addition to mechanical compaction, which reduces porosity, transformation of clay minerals such as smectite and illite also plays an important role because this process releases water and increases pore pressure. As pore pressure gets higher, effective stress becomes lower and seismic velocity decreases. This chapter presents a 2D field data application in which I take advantage of the one to one relationship between pore pressure and velocity to build a model for migration.

Field data application

The relationship between pore pressure and velocity can also be combined with mud weight data to derive bound constraints for FWI. Since pore pressure is bounded

below by hydrostatic pressure and bounded above by mud weights, the velocity converted from hydrostatic pressure in turn becomes the upper bound while the velocity converted from mud weights becomes the lower bound for velocity. Chapter 5 presents an application of constrained anisotropic FWI on a 3D field data from the Gulf of Mexico. The final migrated image after constrained inversion shows improvements in continuity and focusing of reflectors when compared to the image from unconstrained inversion. Significant depth change is also observed between the two images. The common image gathers are better flattened when the constraints are enforced.

GPU implementation and adaptation

Practical applications of anisotropic FWI cannot ignore computational consideration. In Chapter 6 I implement a pipeline algorithm for the time domain finite difference solver on Graphics Processing Units (GPU). This algorithm takes advantage of the locality of the difference stencil to process only a portion of a 3D volume on the device while maintaining complete overlap between data transfer and computation by performing multiple time steppings. This design allows for the propagation of seismic wavefields on an arbitrarily large volume using one single GPU device, thus avoiding domain decomposition, and is very attractive for cloud environments. In addition, with the current GPU memory capacity, extended images, which are conventionally computed on CPU only due to their sheer volume, can now be calculated on GPU.

Appendices

The appendices provide supplementary materials. Appendix A presents a symbolic derivation of wave equation operators. By treating velocity as a scalar variable, the derivation is more compact and easier to understand without loosing mathematical rigor. Appendix B shows how one can break up a two-step recursive relation into two one-step relations and easily derive its adjoint equation. This is important for any wave equations that are second order in time. Appendix C summarizes equations

and parameters for a general visco-elastic anisotropic medium. This can be used to generate independent data for testing FWI algorithms or serve as a reference/starting point for the inversion of elastic parameters and attenuation in future research.

ASSUMPTIONS AND LIMITATIONS

This thesis considers the simplest type of anisotropy, VTI, in which the symmetry axis is vertical and there is no azimuthal velocity variation. Sedimentary layers in real life, however, are commonly tilted and folded. Tilted Transverse Isotropy (TTI) is the next kind of anisotropy to be considered. TTI introduces two more parameters, a polar angle and an azimuth angle, to describe the tilted symmetry axis (Duveneck and Bakker, 2011; Zhang et al., 2011; Fletcher et al., 2009). This increases the number of parameters from *three* for VTI to *five* for TTI. Although these angles could be estimated from the dip angles of reflectors measured on the migrated image, estimating them from seismic data is another challenging problem. To account for azimuthal velocity variation, one needs to incorporate orthorhombic anisotropy, which requires *six* independent parameters for compressional waves.

Compared to an isotropic model, acoustic VTI aniostropy obviously describes seismic waves better and can serve as the first step to build a more complete subsurface model. Real rocks, however, have variable density, behave elastically, and are porous and attenuative. These complex behaviors not only require more compute power to model but also make the inverse problem even more under-determined. These models have been studied in forward seismic modeling and migration. The estimation of subsurface parameters in these settings are subjects of current and future research in the industry.

Ignorance of variable density, elasticity, and attenuation when inverting field data affects the accuracy of inversion results. Estimating the source wavelet and normalizing the seismic traces in the objective function help mitigate the effect (Chapter 5) but really how much the recovered velocity suffers is difficult to measure without performing an elastic inversion.

The rock physics workflow I develop and build the inversion constraints from has its own assumptions and limitations. Discussions of these assumptions are postponed until Chapter 5.